

# A minimal single-channel model for the regularity of beating in the sinoatrial node

Michael R. Guevara and Timothy J. Lewis<sup>a)</sup>

Department of Physiology and Centre for Nonlinear Dynamics in Physiology and Medicine,  
McGill University, Montreal H3G 1Y6, Canada

(Received 30 June 1994; accepted for publication 7 December 1994)

It has been suggested that the normal irregular beating of the heart is a manifestation of deterministically chaotic dynamics. Evidence proffered in support of this hypothesis includes a  $1/f$ -like power spectrum, a small noninteger correlation dimension, and self-similarity of the time series. The major cause of the normal fluctuations in heart rate is the impingement of several neural and hormonal control systems upon the sinoatrial node, the natural pacemaker of the heart. However, intrinsic fluctuations of beat rate can be seen in the isolated node, devoid of all neural and hormonal inputs, and even in a single cell isolated from the node. The electrical activity in such a single cell is generated by ions flowing through discrete channels in the cell membrane. We decided to test the hypothesis that the fluctuations in beat rate in a single cell might be due to the fluctuations in the activity of this population of single channels. We thus assemble a model consisting of 6000 channels and probe its dynamics. Each channel has one or more gates, all of which must be open to allow current to flow through the channel. Since these gates are thought to open and close in a random manner, we model each gate by a Markov process, assigning a pseudorandom number to each gate every time that it changes state from open to closed or vice versa. This number, in conjunction with the classical voltage-dependent Hodgkin–Huxley-like rate constants that control the speed with which a gate will open or close, then determines when that gate will next change state. We also employ a second method that is much more efficient computationally, in which one computes the lifetime of the ensemble of 6000 channels. We show that the Monte Carlo model has behavior consistent with the hypothesis that the irregular beating seen experimentally in single nodal cells is due to the (pseudo)random opening and closing of single channels. However, since the pseudorandom number generator used in the simulations is deterministic, one cannot state that the activity in the model is random (or stochastic). Thus, it would be premature to claim that the irregularity of beating in a single nodal cell is accounted for by the *stochastic* behavior of a population of a few thousand single channels lying in the membrane of the cell. Finally, we consider some implications of our work for the naturally occurring *in situ* fluctuations in heart rate (“heart rate variability”). © 1995 American Institute of Physics.

## I. INTRODUCTION

We are all well aware of the fact that our own hearts do not beat with a perfectly regular rhythm. Three lines of evidence exist that might lead one to speculate that this irregular beating is a manifestation of chaotic dynamics: (i) the correlation dimension of the electrocardiogram is not an integer,<sup>1–3</sup> suggesting the existence of a strange attractor; (ii) there is self-similarity,<sup>4–6</sup> reminiscent of many chaotic systems; and (iii) there is a  $1/f$ -like power spectrum,<sup>4,7</sup> which it is known can occur in intermittency.<sup>8,9</sup> Kobayashi and Musha<sup>7</sup> raised two possibilities for the origin of the  $1/f$  spectrum: it is either intrinsic to electrical activity in the membrane of the sinoatrial node (SAN), the natural pacemaker of the heart, or it is generated by the neural feedback systems that control heart rate. It is at present difficult to realistically model the entire cardiovascular system with its myriad of feedback control loops. It is even difficult to model the isolated SAN, since it is an extended, inhomogeneous structure,<sup>10–12</sup> the details of which are still under investiga-

tion. We therefore decided to formulate a model of a single SAN cell, in which fluctuations in beat rate are produced by the opening and closing of single channels in the cell membrane, in order to ascertain the extent to which these processes, which are presently thought to be random, might account for the irregular beating seen experimentally in single SAN cells.<sup>13–15</sup> We then go on to discuss the relevance of our work for the regularity of beating in the intact heart (“heart rate variability”).

## II. METHODS

There are several ionic models of spontaneous activity in the SAN.<sup>16</sup> We have chosen to use the model of Irisawa and Noma,<sup>17</sup> simplifying it by removing the fast inward sodium current  $I_{Na}$  and the pacemaker current  $I_h$  (more commonly termed  $I_f$ ). This reduced “minimal” model thus has only three currents:  $I_s$  (the slow inward calcium current),  $I_K$  (the delayed rectifier potassium current), and  $I_l$  (the time-independent background or “leak” current). We did not take the further simplifying step of making activation of  $I_s$  time independent.<sup>18</sup>

We use two methods to simulate single-channel dynam-

<sup>a)</sup>Present address: Department of Mathematics, University of Utah, Salt Lake City, Utah 84112.

ics. In both methods, one assumes that gates behave independently of one another, i.e., there is no "cooperativity." In the first method,<sup>19-21</sup> each gate of each channel is treated individually: one can thus refer to it as the "simple" method.<sup>20</sup> We illustrate this approach using the  $I_K$  current, which in the Irisawa-Noma description has but one activation variable (raised to the first power), and no inactivation variable. There is thus only one gate controlling each  $I_K$  channel: when that gate is open, the channel conducts; when it is closed, the channel does not conduct. The activation gate of each  $I_K$  channel has a pseudorandom number (drawn from a uniform distribution on  $(0,1]$ ) assigned to it when it changes state from open to closed or vice versa. The Hodgkin-Huxley-like rate constants  $\alpha_p$  and  $\beta_p$  for the macroscopic  $I_K$  current, which are nonlinear functions of the transmembrane voltage, control the duration that that particular gate will remain in its present configuration (i.e., open or closed). The Hodgkin-Huxley-like equation governing the activation variable  $p$  is

$$\frac{dp}{dt} = \alpha_p(1-p) - \beta_p p. \quad (1)$$

In the traditional interpretation,  $p$  gives the fraction of  $I_K$  activation or "p" gates open at any given time  $t$ . In the simple method, when one is following an individual  $I_K$  channel that opens at time  $t_{\text{open}}$ , one assigns a pseudorandom number  $r$  to the gate at that time. One then numerically integrates until the time  $t_{\text{close}}$  such that

$$-(\ln r) = \int_{t_{\text{open}}}^{t_{\text{close}}} \beta_p [V(t)] dt. \quad (2)$$

At time  $t_{\text{close}}$  the channel flips from the open state to the closed state. A new pseudorandom number is then assigned to the gate, and Eq. (2) is then used once again to compute the time to the next opening of the gate, but with  $\beta_p$  being replaced by  $\alpha_p$  and  $t_{\text{open}}$  and  $t_{\text{close}}$  switched in the limits of the integral. The transmembrane potential  $V$  is computed using forward Euler integration of the equation

$$\frac{dV}{dt} = -(I_s + I_K + I_l)/C, \quad (3)$$

where  $C$  is the cell capacitance, i.e.,  $V(t + \delta t) = V(t) + (dV/dt)\delta t$ , where  $\delta t$  is the integration step size, which is fixed at 0.1 ms in the computations presented below involving the simple method. The smallest activation or inactivation time constant in the range of potentials considered here is the activation time constant of  $I_s$ , which approaches 1 ms at depolarized potentials, and so is an order of magnitude larger than  $\delta t$ .

In the second method (adopted with modification from method 2a of Ref. 19), which we term the "complex" method, one keeps track of the ensemble of channels.<sup>14,15,19,22</sup> We illustrate this method for the case where one has both  $I_s$  and  $I_K$  channels present, and no others. At each step of the numerical procedure, one keeps track of the number of  $I_K$  gates (or equivalently, channels) in each of the two possible states: open ( $N_{Ko}$ ) and closed ( $N_{Kc}$ ). Since it follows from the Irisawa-Noma description of  $I_s$  that there is one activation and one inactivation gate for each

channel, there are four possible states for each  $I_s$  channel. One therefore notes at each step of the procedure the number of  $I_s$  channels in each of these four states:  $N_{scc}$  (activation and inactivation gate both closed),  $N_{sco}$  (activation gate closed, inactivation gate open),  $N_{soc}$  (activation gate open, inactivation gate closed), and  $N_{soo}$  (both activation and inactivation gates open). At time  $t$ , one then calculates a realization of the lifetime  $\Delta t$  of that state of the ensemble from

$$\begin{aligned} \Delta t = & -(\ln r) / [\alpha_p N_{Kc} + \beta_p N_{Ko} + \alpha_d (N_{scc} + N_{sco}) \\ & + \beta_d (N_{soc} + N_{soo}) + \alpha_f (N_{scc} + N_{soc}) \\ & + \beta_f (N_{sco} + N_{soo})], \end{aligned} \quad (4)$$

where  $r$  is a pseudorandom number drawn from a uniform distribution on  $(0,1]$  at time  $t$ ,  $\alpha_d$  and  $\beta_d$  are the rate constants for the activation variable ( $d$ ) of  $I_s$ , and  $\alpha_f$  and  $\beta_f$  are the rate constants for the inactivation variable ( $f$ ) of  $I_s$ . Once  $\Delta t$  is known, one must then decide which of the six possible transitions actually occurs at time  $t + \Delta t$ . This is obtained by calculating the probability of occurrence of each of these transitions [e.g., the probability of the transition being the one in which a closed  $p$  gate opens is given by  $\alpha_p N_{Kc}$  divided by the overall rate constant appearing in the denominator of Eq. (4)]. One then places six intervals next to one another, with lengths corresponding to each of the six probabilities calculated above. By construction, the sum of the lengths of these intervals is one, since one of the six transitions must occur. To decide which transition occurs, one then determines into which of these six intervals a second pseudorandom number drawn from a uniform distribution on  $[0,1]$  falls. Simple forward Euler integration of Eq. (3) is then used to determine  $V(t + \Delta t)$ : i.e.,  $V(t + \Delta t) = V(t) - (I_s + I_K + I_l)\Delta t/C$ .

The error in the complex method is associated with the fact that the voltage is actually changing during the time  $\Delta t$ , and so the rate constants and the assorted probabilities are also changing. One can keep this error within bounds by not allowing the change in voltage during  $\Delta t$  to exceed a certain maximum limit.<sup>19</sup> In our algorithm, when  $V(t + \Delta t)$  exceeds  $V(t)$  by more than 0.4 mV in absolute value,  $\Delta t$  is halved (successively if need be) and the calculations of the currents and  $V(t + \Delta t)$  redone until the desired accuracy is achieved. For continuous Hodgkin-Huxley-like equations (i.e., not for the single-channel model), it can be proven that this time-step-halving algorithm converges.<sup>23</sup> Since the probability of an event occurring in a time  $\Delta t$  is independent of the prior history of the system, one can simply carry out the drawing procedure described above at time  $t + \Delta t$  to continue the simulation, without affecting the validity of the process.<sup>19</sup>

Computations were run in single precision (approximately seven significant decimal digits) on a DECsystem 2100. Programs were written in FORTRAN77 and the system-supplied double precision library subroutine RAND was used to produce pseudorandom numbers to determine open- and closed-times of gates as outlined above.

### III. RESULTS

The Irisawa–Noma model follows the Hodgkin–Huxley formalism, and is thus formally a deterministic system of continuous nonlinear ordinary differential equations. We shall refer to this model as the “continuous” model. From the physiological viewpoint, this type of model corresponds to a situation in which each ionic current flows through an infinite number of channels, each of infinitely small conductance. However, it is now established that there are a finite number of individual channels in the cell membrane, each with a discrete conductance. In what follows, the model constructed as a population of finite-conductance single channels, each opening and closing as time progresses, will be referred to as the “single-channel” model.

The first step in producing the single-channel model from the continuous model is to estimate the number of channels in a single SAN cell. Since  $I_K$  has a linear open-channel current–voltage relationship,<sup>24</sup> one has

$$I_K = P_o N_K \gamma_K (V - E_K), \quad (5)$$

where  $V$  is the transmembrane voltage,  $P_o$  is the probability that the activation gate (and therefore the channel itself) will be open at that voltage,  $N_K$  is the number of  $I_K$  channels,  $\gamma_K$  is the single-channel conductance, and  $E_K$  is the reversal potential for  $I_K$ . An estimate of  $\gamma_K$  of 1.6 pS at physiological external  $[K^+]$  has been made from extrapolation of the results of single-channel voltage-clamp experiments carried out at unphysiologically high values of external  $[K^+]$ .<sup>24</sup> Using Eq. (5)—suitably modified to include a fast inactivation process not included in the Irisawa–Noma model—an estimate of  $N_K$  of  $1054 \pm 254$  ( $n=13$ ) has been made from experiments carried out in cells with an average capacitance of about 35 pF.<sup>24</sup> We use  $N_K=1000$  and  $C=35$  pF in the model below.

The value of  $\gamma_s$  has been estimated to be about 4 pS from noise analysis carried out in small strips cut out of the SAN.<sup>25</sup> We are not aware of any experimentally derived estimates of the number of  $I_s$  channels ( $N_s$ ) in isolated SAN cells. We therefore calculated a value of  $N_s$  that would be appropriate for the Irisawa–Noma model. Since  $I_s$  rectifies in this model, we computed the slope conductance of the fully activated, noninactivated current at its reversal potential of 40 mV, which is positive to where rectification sets in. This leads to a value of  $0.6$  mS  $\text{cm}^{-2}$ . For a single cell capacitance of 35 pF, this results in a single-cell conductance of 21 nS. Given the single-channel conductance of 4 pS, one arrives at  $N_s=5250$ . This results in a channel density of  $1.5$   $\mu\text{m}^{-2}$  (assuming the usual specific capacitance of  $1$   $\mu\text{F cm}^{-2}$ ), which is within the range of  $0.1$ – $5.0$   $\mu\text{m}^{-2}$  reported for neonatal and adult ventricular cells (see Refs. 26 and 27 and references therein). In the model below we use  $N_s=5000$ .

Figure 1(a) shows a voltage-clamp simulation, in which the activation variable  $p$  of  $I_K$  in the continuous model is plotted as a function of time. At  $t=0$  ms,  $p$  is set to zero, corresponding to clamping the transmembrane potential to a very negative value. The voltage is then stepped up to a potential of +50 mV at  $t=0$  ms, producing almost complete activation (i.e.,  $p=1.0$ ) of the current, and then down to  $-50$

mV at  $t=2000$  ms. The variable in the single-channel model corresponding to  $p$  is the fraction of  $I_K$  channels open. Figure 1(b) shows this fraction for the case when the cell has 1000  $I_K$  channels, which is the number used in our single-cell model. Figures 1(c) and 1(d) show the results when the number of  $I_K$  channels ( $N_K$ ) is reduced to 100 and then further to 10. Note the increase in the “noise,” especially visible upon clamping down to  $V=-50$  mV.

Figure 2 shows a voltage-clamp protocol carried out in the single-channel model ( $N_K=1000$ ) in which the voltage is first stepped to a clamp potential of 0,  $-20$ , or  $-40$  mV at  $t=0$  ms to activate  $I_K$ , followed by a step down to  $-50$  mV at  $t=2500$  ms to deactivate the current. As expected, one sees effects due to the voltage dependence of steady-state activation and the time constant of activation. The trace at the bottom of the figure shows a record of the activity in one of the thousand  $I_K$  channels upon clamping to 0 mV. It is clear that the mean open time is larger at the more depolarized clamp potential than at the more hyperpolarized holding potential.

Figure 3(a) shows the transmembrane potential as a function of time in the deterministic three-current minimal Irisawa–Noma model. The trace is smooth, since, as already mentioned, it is produced by a continuous system of differential equations. Figure 3(f) shows the corresponding trace produced by the single-channel model, with channel numbers as estimated above (5000 for  $I_s$ , 1000 for  $I_K$ ). Note the more irregular look of the trace, especially during the pacemaker potential. Figures 3(b) and 3(g) show the total current ( $I_{\text{tot}}$ ) in the two models, while Figs. 3(c) and 3(h) give the individual currents. In the single-channel model, the background current ( $I_l$ ) is left in its continuous Hodgkin–Huxley form (see Sec. IV). Note that the fluctuations visible in  $I_K$  in Fig. 3(h) are considerably smaller in amplitude than those in  $I_s$ . Figure 3(i) shows the fraction of  $I_K$  and  $I_s$  channels open in the single-channel model, while Fig. 3(d) gives the analogous traces ( $p$  and  $df$ , respectively) in the deterministic model. Figure 3(j) shows the fraction of the  $d$  ( $I_s$  activation) and  $f$  ( $I_s$  inactivation) gates open. (The fraction of  $I_K$  channels open [Fig. 3(i)] also gives the fraction of  $p$  gates open.) These three traces of the fractions of  $d$ ,  $f$ , and  $p$  gates open [Figs. 3(i) and 3(j)] show time courses similar to those of the activation and inactivation variables ( $d, f, p$ ) in the deterministic model [Figs. 3(d) and 3(e)]. While the amplitudes of the fluctuations in the numbers of  $I_s$  and  $I_K$  channels open [Fig. 3(i)] are roughly comparable, there seem to be larger fluctuations in the number of  $d$  gates open than in the number of  $f$  gates open [Fig. 3(j)]. In this 750 ms run, the  $d$ ,  $f$ , and  $p$  gates open and close about  $10^5$ ,  $2 \times 10^4$ , and  $10^3$  times, respectively. Thus the mean value of the lifetime  $\Delta t$  of the ensemble of channels [Eq. (4)] is about  $6$   $\mu\text{s}$ .

Figure 4(a) shows 10 s of spontaneous activity in the single-channel model. The first cycle of this activity was shown earlier in Fig. 3(f) on an expanded time scale. Figure 4(b) is a tachogram, giving the  $i$ th interbeat interval ( $\text{IBI}_i$ ) as a function of interval number ( $i$ ), calculated from a 50 s long simulation. A joint interval distribution<sup>28</sup> or scattergram of this data, in which each  $\text{IBI}$ —apart from the first—is plotted versus the preceding  $\text{IBI}$  is presented in Fig. 4(c). The inter-

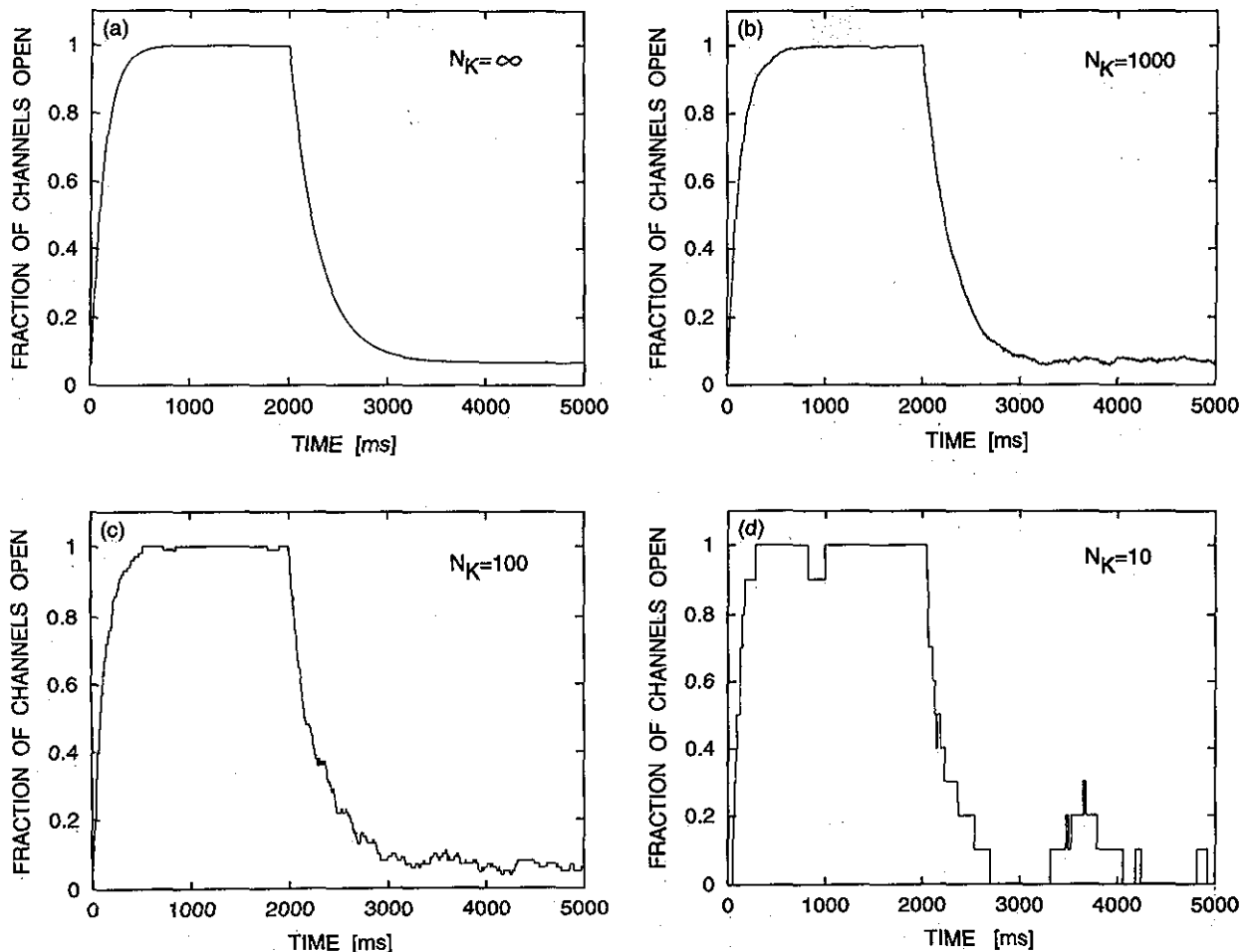


FIG. 1. Simulation of voltage-clamp step. All  $I_K$  channels closed at  $t=0$ , at which time  $V$  is stepped to 50 mV. At  $t=2000$  ms, a step down to  $-50$  mV is made. (a) Continuous Hodgkin-Huxley-like model. (b)–(d) Single-channel model with 1000 (b), 100 (c), and 10 (d)  $I_K$  channels. In (a)–(d), integration step size is 0.1 ms, and data points are plotted every 1 ms. In (b)–(d), “simple” simulation method is used.

val histogram<sup>29</sup> is shown in Fig. 4(d), while the serial correlation coefficients ( $R_j$ ) are shown in Fig. 4(e).<sup>15,30,31</sup> Note the rapid decline in the  $R_j$ . The persistence of positive small nonzero values for  $j \geq 1$  is due to the slow drifts in IBI evident in Fig. 4(b).<sup>30</sup> Scrambling the IBIs with a pseudorandom number generator results in the  $R_j$  oscillating equally positive and negative about the zero baseline (see also Fig. 2-2 of Ref. 31). This rapid decline to zero for  $j > 1$  shows the lack of dependence of any given IBI on the preceding IBIs.

Figure 4 showed results for one simulation run, starting out with a particular seed value for the pseudorandom number generator. Figure 5 shows IBIs for four other runs, each starting out with a different seed value. While it is apparent that the details of each run are quite different, the mean IBI of the five-run ensemble is 398 ms and the mean coefficient of variation (standard deviation divided by mean) of IBI for the ensemble is 3.8%. This ensemble mean IBI is extremely close to the value of 395 ms obtained in the continuous model [Fig. 3(a)], using a variable time-step algorithm with an identical upper limit (0.4 mV) on the change in voltage allowed during one integration time step.<sup>32</sup>

When  $N_s$  and  $N_K$  are decreased by a factor of 10 (to 500

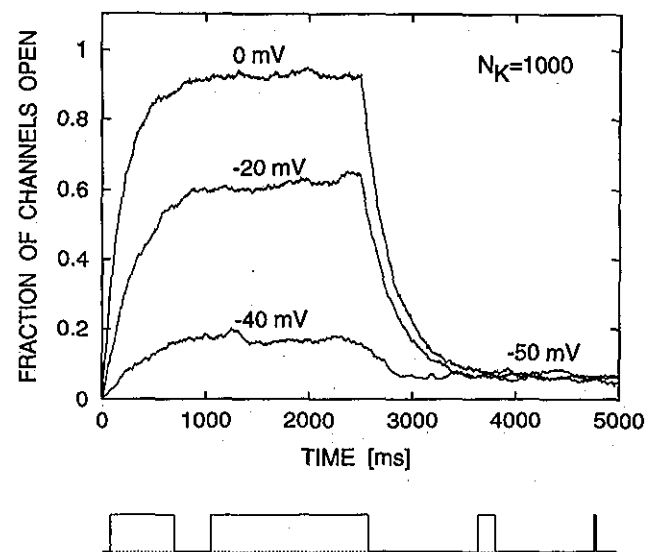


FIG. 2. Top: Simulation of voltage clamp step in single-channel model of 1000  $I_K$  channels. All  $I_K$  channels are closed at  $t=0$ , at which time  $V$  is stepped to 0,  $-20$ , or  $-40$  mV, and then down to  $-50$  mV at  $t=2500$  ms. Bottom: Time series from one of the 1000 channels during the simulation involving the step to 0 mV. The “simple” simulation method was used, with 0.1 ms integration step size, and data points plotted every 1 ms.

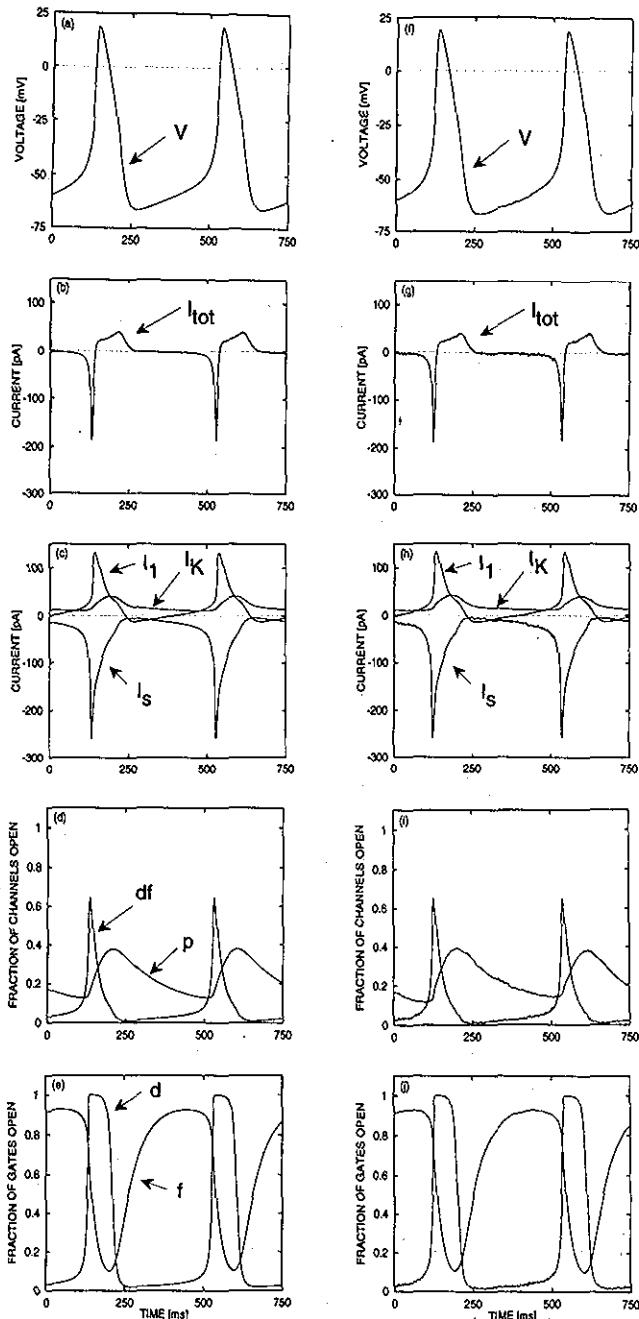


FIG. 3. 750 ms run of spontaneous activity in continuous (left panel) and single-channel (right panel) models. (a),(f)  $V$ ; (b),(g)  $I_{tot}$ ; (c),(h)  $I_s, I_K, I_I$ ; (d)  $df, p$ ; (i) fractions of  $I_s, I_K$  channels open; (e)  $d, f$ ; (j) fractions of  $d, f$  gates open. Initial conditions (left panel):  $V = -60$  mV,  $d = 0.003$  115 67,  $f = 0.910$  749,  $p = 0.171$  578. Initial conditions (right panel):  $V = -60$  mV, fractions of gates open correspond to initial conditions on  $d, f, p$  as stated for the left panel. Not all data points computed are plotted. The "complex" simulation method was used in the right panel.

and 100, respectively), with tenfold increase in single-channel conductance so as to leave the total conductance unchanged, there is a marked increase in the irregularity of beating, with the coefficient of variation of the IBI increasing to about 12%.

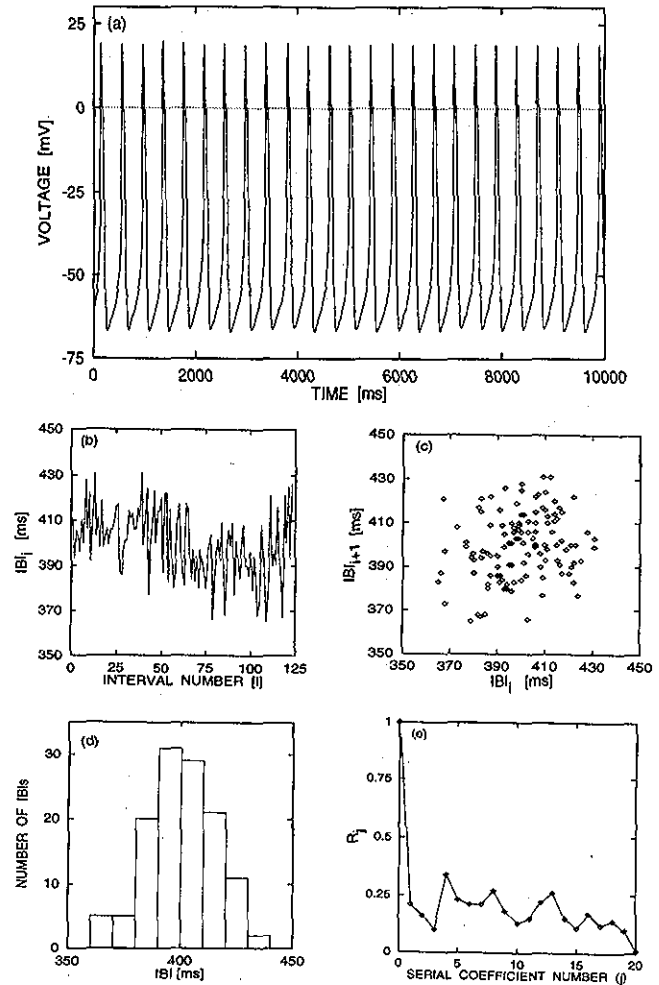


FIG. 4. 50 s run of spontaneous activity in the single-channel model. (a) First 10 s of transmembrane potential. (b) Tachogram. (c) IBI scattergram. (d) IBI histogram. (e) IBI serial correlation coefficients. Mean IBI = 400 ms, coefficient of variation of IBI = 3.7%. Same initial conditions as in Fig. 3. In (a), not all computed data points are plotted. Computation time for 50 s run is about 20 min. "Complex" simulation method is used.

## IV. DISCUSSION

### A. Comparison with experimental data

In healthy human subjects the coefficient of variation for a run of between 25 and a few hundred heart beats is on the order of 10%–15%.<sup>33,34</sup> In 36 h recordings from isolated rat hearts, the coefficient of variation also seems to be of about the same magnitude.<sup>35</sup> In the isolated rabbit SAN, the coefficient of variation for one 300-beat run was much smaller, being about 0.4%.<sup>36</sup> Since the isolated SAN is a population oscillator consisting of many coupled cells, one would expect it to be considerably more regular than a single SAN cell.<sup>36,37</sup> This is indeed the case: in runs ranging from 34 to 136 beats in 14 single SAN cells, the coefficient of variation ranged between 1.4% and 2.8%, averaging 2.0%.<sup>15</sup> The value obtained in our model of 3.8% [Figs. 4(b) and 5] is thus about double this experimental value. The most obvious candidate to account for this discrepancy is an underestimation of one or more of the numbers of single channels and/or overestimation of the single-channel conductance(s). A

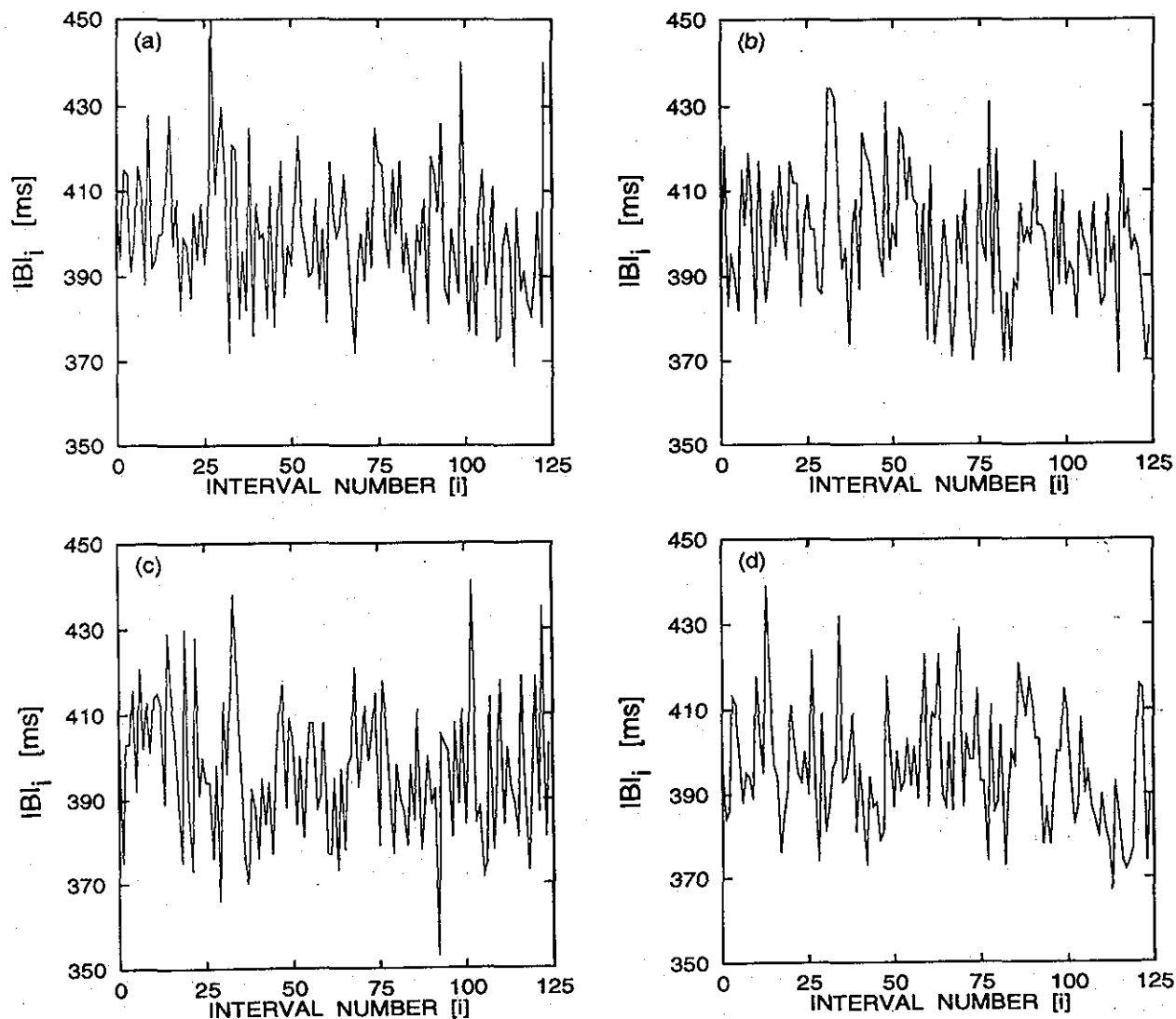


FIG. 5. Tachograms resulting from four simulation runs in the single-channel model, starting with different seeds for the pseudorandom number generator. Mean IBI and coefficient of variation of IBI: (a) 400 ms, 3.9%; (b) 399 ms, 3.8%; (c) 397 ms, 4.1%; (d) 396 ms, 3.6%. "Complex" simulation method is used.

simple random-walk-to-threshold model of the pacemaker potential predicts that the coefficient of variation of IBI should be inversely proportional to the square-root of the number of channels present in the membrane.<sup>37</sup> Coupling together several "stochastic" SAN cells produces a result consistent with this estimate.<sup>14</sup> Thus one would expect that increasing the number of  $I_s$  channels from our standard value of 5000 to 10 000 should lead to a coefficient of variation of about 2.7%. While this is indeed exactly what one finds in the model, this value lies at the upper end of the range of reported experimental values. In a recent report involving a more detailed SAN model,<sup>16</sup> in which the estimated number of  $I_s$  channels is 10 000, the mean coefficient of variation for three 100-beat runs was found to be 2.2%.<sup>15</sup> Our conclusion from the above results is that the single-channel fluctuations in the two currents  $I_s$  and  $I_K$  suffice to account for the major part of the fluctuations in IBI experimentally observed in single SAN cells.

## B. Problems with the single-channel model

In the Irisawa–Noma model, both  $I_K$  and  $I_s$  rectify. In the simulations presented above, we have treated the rectification as residing in the single-channel conductance: i.e., we have made the conductance of the open channel (i.e., the single-channel conductance) a function of voltage. However, the  $I_K$  channel is linear in nodal cells,<sup>24</sup> and it is a relatively fast voltage-dependent inactivation process that lies at the root of the rectification.<sup>24</sup> Since this inactivation process is not included in the Irisawa–Noma description of  $I_K$ , we did not include it in our model. In addition, the Irisawa–Noma equations for  $I_K$  were derived from voltage-clamp experiments carried out on the rabbit SAN. In the guinea-pig SAN, the major component of  $I_K$  present is not  $I_{K,r}$ , but rather  $I_{K,s}$ .<sup>38</sup>

While  $I_s$  rectifies in the SAN,<sup>39</sup>  $I_s$  channels have a linear current–voltage relationship in ventricular cells.<sup>27</sup> To make

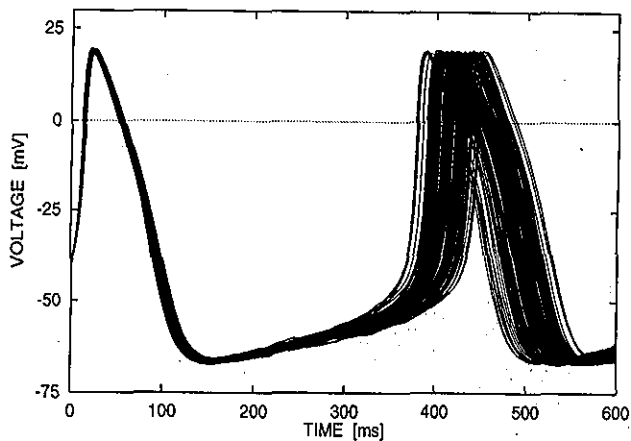


FIG. 6. Superimposed cycles from 50 s run, the first 10 s of which was shown in Fig. 4(a). Cycles all start off at  $t=0$  when  $V$  crosses  $-40$  mV on the action potential upstroke.

matters far worse, the simple four-state kinetic scheme for  $I_s$  used here is probably an oversimplification in the SAN, since  $I_s$  channels have much more esoteric kinetics in ventricular cells, including bursting due to the presence of multiple closed states.<sup>26</sup> Thus, future work will be needed to explore how the rectification, multiple closed-state properties, and species differences change the results presented above.

We have not formulated the background current  $I_l$  of the Irisawa–Noma model as a population of single channels since we do not feel that it is realistic to do so at the present time. First of all, the ionic nature of the background current in the SAN is still undetermined. A chloride-sensitive current has been described,<sup>40</sup> and more recent work describes a current carried by both  $\text{Na}^+$  and  $\text{K}^+$  ions.<sup>41</sup> In neither case has the single-channel conductance been reported. Second, the  $I_l$  current in the Irisawa–Noma model is presumably a sum of these (and perhaps other yet to be determined) background currents, as well as other currents, such as the  $\text{Na}^+$ – $\text{K}^+$  pump current. Thus we feel that it is premature to include these currents in a single-channel model.

### C. Implications for the intact SAN

There are two major problems in extrapolating the above results to the intact SAN. First, SAN cells form an inhomogeneous population (see Ref. 42 for a recent review of the ionic currents in SAN cells), with, for example, some cells possessing much more  $I_{\text{Na}}$ ,<sup>11,43</sup>  $I_h$ ,<sup>44</sup> or  $I_{\text{Ca,T}}$  (Ref. 45) than others. This inhomogeneity is reflected in the fact that even simple visual inspection of the records of spontaneous activity in single cells shows differences in the origin of the IBI fluctuations: e.g., fluctuation in action potential duration can account for anywhere between 20% and 50% of the IBI fluctuation in different cells (see Fig. 1 of Ref. 13, Figs. 4.1 and 4.5 of Ref. 14). In our model, only a small part (roughly 20%) of the IBI fluctuation is traceable to fluctuations in action potential duration (Fig. 6). While our minimal model might be a reasonably good caricature of cells from the central part of the SAN, cells from the more peripheral parts of the node can possess significant amounts of  $I_{\text{Na}}$  and  $I_f$ . It

remains to be seen what happens to the regularity of beating in single-channel models of cells that depend on  $I_{\text{Na}}$  and/or  $I_f$  for generation of spontaneous activity. The unusually small single-channel conductance of  $I_f$  (Ref. 46) might result in more regular beating in cells that depend upon  $I_f$  for pace-making.

A second problem is that the coupling between cells in the SAN is anisotropic and highly inhomogeneous,<sup>47</sup> with much better coupling in the periphery than in the center.<sup>10</sup> The implications for this in terms of the regularity of beating in a population oscillator remain unexplored. In addition, the gap-junctional channels that provide this cell-to-cell coupling themselves gate in a stochastic manner.<sup>14</sup>

### D. Random or chaotic?

*“Anyone who considers arithmetical methods of producing random digits is, of course, in a state of sin”* [J. von Neumann (1951), quoted in Ref. 48].

The above computations show that the fluctuations in IBI in a model formulated as a population of single channels is consistent with the experimental data. Thus, it is unlikely that chaos would have any role in generating the irregular beating of isolated cells, unless one could replace the stochastic interpretation of the kinetics of single channels with a chaotic one.<sup>49,50</sup> Unfortunately, there is at the present time no foolproof way of deciding whether the opening and closing of a single channel (i.e., an experimental record corresponding to the simulation shown in the lower part of Fig. 2) is deterministically chaotic or stochastic.

In addition, there is another consideration. A system-supplied pseudorandom number generator subroutine is used in the simulations presented above. This algorithm is deterministic, *not* random or stochastic, since one always obtains the same sequence if one starts with the same seed value. This routine belongs to the class of linear congruential generators which have at their heart a piecewise-linear one-dimensional finite-difference equation of the form

$$I_{i+1} = MI_i + N \pmod{m}, \quad (6)$$

where  $I_i$  is the  $i$ th random integer generated, and  $M$ ,  $N$ , and  $m$  are well-chosen integer constants, with  $M, N \geq 1$ ,  $m \geq 0$ .<sup>48,51,52</sup> For  $N=0$ , one speaks of a (pure) multiplicative congruential generator. For judicious choices of the constants in Eq. (6), the deterministic sequence of integers produced has a very long repetition period, low serial correlation, and passes many of the statistical tests of randomness.<sup>48,51,52</sup> However, for  $M > 1$ , the real (in contrast to integer) counterpart of Eq. (6) generates chaotic behavior.<sup>53</sup> Thus one can make the argument—even in the case of exact integer arithmetic implementation on a computer, with no roundoff or truncation errors—that the output of Eq. (6) has more in common with a chaotic process than with a stochastic one.

A single-channel model of squid axon membrane replicates much of the irregular appearance of experimental traces that are claimed to be chaotic.<sup>54</sup> However, since that single-channel model presumably used a deterministic pseudorandom number generator, the conclusion that a *stochastic* single-channel population mechanism can account for the irregularity seen in the experimental traces is premature. Simi-

lar remarks hold for single-channel models of bursting pancreatic  $\beta$  cells (see Sec. IV F). Nevertheless, it is unlikely that the interpretation of the results of these simulations would be changed, in terms of their characterization using simple phenomenological measures, should the pseudorandom sequence be replaced with a sequence of numbers that would be universally accepted as being truly random (e.g., one obtained from radioactive decay or a noise diode<sup>48</sup>). Indeed, it is unlikely that any presently available technique would be able to discriminate between the two sets of simulations, given the output voltage tracing from the model as input data.

The opening or closing of a channel, which is a protein, is usually taken as being caused by a conformational change in that molecule, which is governed by the laws of quantum mechanics. Thus, as previously stated,<sup>31</sup> deterministically nonperiodic dynamics can only occur in single channels should the Copenhagen (statistical) interpretation of quantum mechanics be replaced by a deterministic mechanism. While Einstein's opposition to the Copenhagen interpretation is oft cited ("God does not play dice with the universe"),<sup>55</sup> one can also adopt the view—formulated in a recent study of whether the toss of a die is chaotic—that "even if a process in principle is deterministic, we may consider it as random if the complexity involved is so high that we cannot relate cause and effect in detail."<sup>56</sup> Or perhaps, more poetically stated: "In a sense, randomness, like beauty, is in the eye of the beholder."<sup>52</sup>

### E. Heart rate variability: Chaos in the intact heart?

Our study does not rule out the possibility that chaotic activity might occur in the beating of an isolated SAN cell over the long term (e.g., due to the presence of intracellular biochemical feedback mechanisms with time delays). Chaos might equally well occur, even in the short term, when many individually oscillating pacemaker cells are coupled together to form an intact isolated SAN. There are many intracardiac feedback mechanisms (e.g., stretch of the SAN caused by pulsation of the sinoatrial nodal artery) that operate to control nodal rate,<sup>57</sup> as well as numerous neural and hormonal regulatory systems. These systems all depend on ion-channel gating and neurotransmitter release for their action, and hence have stochastic components. Their characteristic response times range from less than a second (e.g., the baroreceptors) to days (e.g., control of blood volume by the kidney), and their feedback gains span many orders of magnitude.<sup>58</sup> It is thus not surprising that IBI<sup>4,7</sup> and blood pressure<sup>59</sup> have broadband power spectra. In addition, ultradian frequency components have been described in heart rate and blood pressure of intact animals,<sup>60</sup> and in the beat rate of isolated hearts.<sup>35</sup> In respiration, where self-similar phenomenology has also been described,<sup>61</sup> there are several discrete components in the power spectrum with frequencies ranging over more than two orders of magnitude.<sup>62</sup>

A decrease in heart rate variability (HRV) has been reported in several disease states, including diabetes,<sup>63</sup> injury to the central nervous system,<sup>64</sup> and congestive heart failure.<sup>65</sup> Decreased HRV predicts a greater mortality after myocardial infarction<sup>66</sup> as well as an increased chance of

sudden cardiac death in patients with coronary heart disease.<sup>34</sup> In obstetrics, loss of HRV in the fetal tachogram is a dire prognostic sign,<sup>67</sup> and, at the other end of life, HRV decreases with age.<sup>63,68,69</sup> In essential hypertension, several studies report a decrease in HRV (see Ref. 33 and references given in Ref. 70), while at least one study reports unchanged HRV.<sup>71</sup> Assuming that fluctuations in heart rate are due to some underlying chaotic mechanism, it is thus tempting to raise the question: "Is it healthy to be chaotic?"<sup>72</sup> However, while HRV might be reduced in hypertension, blood pressure (BP) variability is increased (see references in Ref. 70). Thus, while one could take the decreased HRV variability as a sign of disease in the hypertensive individual, one could equally well conclude from the increased BP variability that the hypertensive individual is in fact "healthier" than the normotensive individual. A similar remark holds for the concomitant decrease in HRV and increase in BP variability with age.<sup>63,68,69,71</sup>

When studying any control system, one should always keep in the back of one's mind consideration of which variable is the controlled variable. The major system for short term regulation of the arterial BP is the carotid baroreceptor reflex. Removal of this "buffer" reflex leads to a great increase in BP variability, but a fall in HRV.<sup>58,73</sup> Individuals (normal or hypertensive) who have a higher baroreceptor reflex gain (slope of line relating IBI to systolic BP) have a lower BP variability, but a higher HRV.<sup>70,74</sup> The conclusion must be that one is observing the response of a controller that is attempting to *reduce* variability in blood pressure (the controlled variable), at the unavoidable expense of increasing variability in heart rate (an effector branch of the feedback loop). In fact, reverting to a perhaps old-fashioned interpretation of the concept of homeostasis, one could make the case that the body is in fact trying to produce a steady state in the blood pressure.

The baroreceptor feedback loop could conceivably be the origin of the  $1/f$  spectrum in IBI,<sup>4,7</sup> since there is a  $1/f$  falloff in the spectrum of the blood pressure waveform.<sup>59</sup> Indeed, in an isolated heart preparation—in which there are no extra-cardiac regulating systems present—the IBI spectrum could not be "reasonably" fit to a power law during normal conditions.<sup>75</sup>

### F. Other applications of the single-channel model

There are several other situations in cardiac electrophysiology in which the single-channel form of the model might be useful in investigating effects to which membrane noise might contribute.<sup>49</sup> e.g., the beat-to-beat fluctuations in action potential duration during 1:1 rhythm in paced isolated ventricular cells, irregular Wenckebach rhythms in isolated ventricular cells,<sup>49</sup> irregular "chaotic" dynamics in periodically stimulated cells,<sup>76,77</sup> Shil'nikov chaos occurring in the Irisawa–Noma model,<sup>32</sup> and annihilation of activity in spontaneously beating preparations.<sup>78</sup> Finally, there are many other noncardiac situations in which chaotic activity has been claimed to exist and in which we believe approaches similar to single-channel modeling will be useful: e.g., bursting activity in pancreatic  $\beta$ -cells,<sup>79,80</sup> rhythmic activity in smooth muscle (e.g., in gut, arterioles, and uterus), intracel-



lular calcium oscillations, neurotransmitter release at nerve terminals (e.g., resulting in the EEG), and pulsatile release of hormones by neurons.

## ACKNOWLEDGMENTS

We thank D. Kaplan for helpful discussions on pseudo-random number generators, J. Outerbridge and A. Yehia for help with computers, and C. Pamplin for help in typing the manuscript. This work was supported by an operating grant from the Medical Research Council (MRC) of Canada. The initial part of this work was carried out by T. Lewis as his senior-year undergraduate research project (1986–87).

- <sup>1</sup>A. Babloyantz and A. Destexhe, "Is the normal heart a periodic oscillator?," *Biol. Cybern.* **58**, 203–211 (1988).
- <sup>2</sup>J. P. Zbilut, G. Mayer-Kress, and K. Geist, "Dimensional analysis of heart rate in heart transplant recipients," *Math. Biosci.* **90**, 49–70 (1988).
- <sup>3</sup>G. Mayer-Kress, F. E. Yates, L. Benton, M. Keidel, W. Tirsch, S. J. Poppl, and K. Geist, "Dimensional analysis of nonlinear oscillations in brain, heart and muscle," *Math. Biosci.* **90**, 155–182 (1988).
- <sup>4</sup>J. P. Saul, P. Albrecht, R. D. Berger, and R. J. Cohen, "Analysis of long term heart rate variability: Methods,  $1/f$  scaling and implications," in *IEEE Computers in Cardiology* (IEEE Computer Society, Silver Spring, 1987), pp. 419–422.
- <sup>5</sup>A. L. Goldberger, D. R. Rigney, and B. J. West, "Chaos and fractals in human physiology," *Sci. Am.* **262**(2), 42–49 (1990).
- <sup>6</sup>N. A. J. Gough, "Fractals, chaos, and fetal heart rate," *Lancet* **339**, 182–183 (1992).
- <sup>7</sup>M. Kobayashi and T. Musha, " $1/f$  fluctuation of heartbeat period," *IEEE Trans. Biomed. Eng.* **BE-29**, 456–457 (1982).
- <sup>8</sup>P. Manneville, "Intermittency, self-similarity and  $1/f$  spectrum in dissipative dynamical systems," *J. Phys.* **41**, 1235–1243 (1980).
- <sup>9</sup>I. Procaccia and H. Schuster, "Functional renormalization-group theory of universal  $1/f$  noise in dynamical systems," *Phys. Rev. A* **28**, 1210–1212 (1983).
- <sup>10</sup>W. K. Bleeker, A. J. C. Mackaay, M. Masson-Pévet, L. N. Bouman, and A. E. Becker, "Functional and morphological organization of the rabbit sinus node," *Circ. Res.* **46**, 11–22 (1980).
- <sup>11</sup>D. Kreitner, "Electrophysiological study of the two main pacemaker mechanisms in the rabbit sinus node," *Cardiovasc. Res.* **19**, 304–318 (1985).
- <sup>12</sup>I. Kodama and M. R. Boyett, "Regional differences in the electrical activity of the rabbit sinus node," *Pflügers Arch.* **404**, 214–226 (1985).
- <sup>13</sup>T. Ophof, A. C. G. van Ginneken, L. N. Bouman, and H. J. Jongsma, "The intrinsic cycle length in small pieces isolated from the rabbit sinoatrial node," *J. Mol. Cell. Cardiol.* **19**, 923–934 (1987).
- <sup>14</sup>R. Wilders, "From single channel kinetics to regular beating," Doctoral thesis, University of Amsterdam, Amsterdam, 1993.
- <sup>15</sup>R. Wilders and H. J. Jongsma, "Beating irregularity of single pacemaker cells isolated from the rabbit sinoatrial node," *Biophys. J.* **65**, 2601–2613 (1993).
- <sup>16</sup>R. Wilders, H. J. Jongsma, and A. C. G. van Ginneken, "Pacemaker activity of the rabbit sinoatrial node. A comparison of mathematical models," *Biophys. J.* **60**, 1202–1216 (1991).
- <sup>17</sup>H. Irisawa and A. Noma, "Pacemaker mechanisms of rabbit sinoatrial node cells," in *Cardiac Rate and Rhythm*, edited by L. N. Bouman and H. J. Jongsma (Martinus Nijhoff, The Hague, The Netherlands, 1982), pp. 35–51.
- <sup>18</sup>M. R. Guevara, A. C. G. van Ginneken, and H. J. Jongsma, "Patterns of activity in a reduced ionic model of a cell from the rabbit sinoatrial node," in *Chaos in Biological Systems*, edited by H. Degn, A. V. Holden, and L. F. Olsen (Plenum, London, 1987), pp. 5–12.
- <sup>19</sup>E. Skaugen and L. Walløe, "Firing behavior in a stochastic nerve membrane model based upon the Hodgkin–Huxley equations," *Acta Physiol. Scand.* **107**, 343–363 (1979).
- <sup>20</sup>J. R. Clay and L. J. DeFelice, "Relationship between membrane excitability and single channel open–close kinetics," *Biophys. J.* **42**, 151–157 (1983).
- <sup>21</sup>L. J. DeFelice and J. R. Clay, "Membrane current and membrane potential from single-channel kinetics," in *Single-Channel Recording*, edited by B. Sakmann and E. Neher (Plenum, New York, 1983), pp. 323–342.
- <sup>22</sup>W. van Meerwijk, "Qualitative models for cardiac pacemakers and their interaction," Doctoral thesis, Leiden University, Leiden, 1988.
- <sup>23</sup>B. Victorri, A. Vinet, F. A. Roberge, and J.-P. Drouhard, "Numerical integration in the reconstruction of cardiac action potentials using Hodgkin–Huxley-type models," *Comput. Biomed. Res.* **18**, 10–23 (1985).
- <sup>24</sup>T. Shibasaki, "Conductance and kinetics of delayed rectifier potassium channels in nodal cells of the rabbit heart," *J. Physiol. (London)* **387**, 227–250 (1987).
- <sup>25</sup>W. Osterrieder, Q.-F. Yang, and W. Trautwein, "Conductance of the slow inward channel in the rabbit sinoatrial node," *Pflügers Arch.* **394**, 85–89 (1982).
- <sup>26</sup>A. Cavalié, D. Pelzer, and W. Trautwein, "Fast and slow gating behavior of single calcium channels in cardiac cells. Relation to activation and inactivation of calcium-channel current," *Pflügers Arch.* **406**, 241–258 (1986).
- <sup>27</sup>T. F. McDonald, A. Cavalié, W. Trautwein, and D. Pelzer, "Voltage-dependent properties of macroscopic and elementary calcium channel currents in guinea pig ventricular myocytes," *Pflügers Arch.* **406**, 437–448 (1986).
- <sup>28</sup>M. ten Hoopen and J. P. M. Bongaarts, "Probabilistic characterization of R-R intervals," *Cardiovasc. Res.* **3**, 218–226 (1969).
- <sup>29</sup>D. W. Simborg, R. S. Ross, K. B. Lewis, and R. H. Shepard, "The R-R interval histogram," *J. Am. Med. Assoc.* **197**, 145–148 (1966).
- <sup>30</sup>D. H. Perkel, G. L. Gerstein, and G. P. Moore, "Neuronal spike trains and stochastic point processes. I. The single spike train," *Biophys. J.* **7**, 391–418 (1967).
- <sup>31</sup>M. R. Guevara, "Chaotic cardiac dynamics," Doctoral thesis, McGill University, Montreal, 1984.
- <sup>32</sup>M. R. Guevara and H. J. Jongsma, "Three ways of abolishing automatically in sinoatrial node: ionic modeling and nonlinear dynamics," *Am. J. Physiol.* **262**, H1268–H1286 (1992).
- <sup>33</sup>R. J. Bagshaw, A. Fronek, L. H. Peterson, and H. F. Zinsser, "Dispersion of blood pressure and heart rate in essential hypertension," *IEEE Trans. Biomed. Eng.* **BE-22**, 508–512 (1975).
- <sup>34</sup>G. J. Martin, N. M. Magid, G. Myers, P. S. Barnett, J. W. Schaad, J. S. Weiss, M. Lesch, and D. H. Singer, "Heart rate variability and sudden death secondary to coronary artery disease during ambulatory electrocardiographic monitoring," *Am. J. Cardiol.* **60**, 86–89 (1987).
- <sup>35</sup>G. D. Tharp and G. E. Folk, Jr., "Rhythmic changes in rate of the mammalian heart and heart cells during prolonged isolation," *Comp. Biochem. Physiol.* **14**, 255–273 (1965).
- <sup>36</sup>H. J. Jongsma and L. Tsjernina, "Factors influencing regularity and synchronization of beating of tissue cultured heart cells," in *Cardiac Rate and Rhythm*, edited by L. N. Bouman and H. J. Jongsma (Martinus Nijhoff, The Hague, The Netherlands, 1982), pp. 397–414.
- <sup>37</sup>J. R. Clay and R. L. DeHaan, "Fluctuations in interbeat interval in rhythmic heart-cell clusters. Role of membrane voltage noise," *Biophys. J.* **28**, 377–389 (1979).
- <sup>38</sup>J. M. B. Anumonwo, L. C. Freeman, W. M. Kwok, and R. S. Kass, "Delayed rectification in single cells isolated from guinea pig sinoatrial node," *Am. J. Physiol.* **262**, H921–H925 (1992).
- <sup>39</sup>A. Noma, H. Kotake, S. Kokubun, and H. Irisawa, "Kinetics and rectification of the slow inward current in the rabbit sinoatrial node cell," *Jpn. J. Physiol.* **31**, 491–500 (1981).
- <sup>40</sup>I. Seyama, "Characteristics of the anion channel in the sino-atrial node cell of the rabbit," *J. Physiol. (London)* **294**, 447–460 (1979).
- <sup>41</sup>N. Hagiwara, H. Irisawa, H. Kasanuki, and S. Hosoda, "Background current in sino-atrial node cells of the rabbit heart," *J. Physiol. (London)* **448**, 53–72 (1992).
- <sup>42</sup>H. Irisawa, H. F. Brown, and W. Giles, "Cardiac pacemaking in the sinoatrial node," *Physiol. Rev.* **73**, 197–227 (1993).
- <sup>43</sup>H. I. Oei, A. C. G. van Ginneken, H. J. Jongsma, and L. N. Bouman, "Mechanisms of impulse generation in isolated cells from the rabbit sinoatrial node," *J. Mol. Cell. Cardiol.* **21**, 1137–1149 (1989).
- <sup>44</sup>J. C. Denyer and H. F. Brown, "Rabbit sino-atrial node cells: isolation and electrophysiological properties," *J. Physiol. (London)* **428**, 405–424 (1990).
- <sup>45</sup>N. Hagiwara, H. Irisawa, and M. Kameyama, "Contribution of two types of calcium currents to the pacemaker potentials of rabbit sino-atrial node cells," *J. Physiol. (London)* **395**, 233–253 (1988).
- <sup>46</sup>D. DiFrancesco, "Characterization of single pacemaker channels in cardiac sino-atrial node cells," *Nature (London)* **324**, 470–473 (1986).

- <sup>47</sup>J. J. Duivenvoorden, "Electrotonic current spread in the rabbit sinoatrial node," Doctoral thesis, University of Amsterdam, Amsterdam, 1989.
- <sup>48</sup>J. Moshman, "Random number generation," in *Mathematical Methods for Digital Computers*, edited by A. Ralston and H. S. Wilf (Wiley, New York, 1967), Vol. II, pp. 249–263.
- <sup>49</sup>M. R. Guevara, "Mathematical modeling of the electrical activity of cardiac cells," in *Theory of Heart*, edited by L. Glass, P. Hunter, and A. McCulloch (Springer-Verlag, New York, 1991), pp. 239–253.
- <sup>50</sup>L. S. Liebovitch and T. I. Toth, "A model of ion channel kinetics using deterministic chaotic rather than stochastic processes," *J. Theor. Biol.* **148**, 243–267 (1991).
- <sup>51</sup>D. E. Knuth, *The Art of Computer Programming* (Addison-Wesley, Reading, MA, 1969), Vol. 2.
- <sup>52</sup>S. K. Park and K. W. Miller, "Random number generators: a good one is hard to find," *Commun. ACM* **31**, 1192–1201 (1988).
- <sup>53</sup>S. Oishi and H. Inoue, "Pseudo-random number generators and chaos," *Trans. IECE Jpn.* **65**, 534–541 (1982).
- <sup>54</sup>L. J. DeFelice and A. Isaac, "Chaotic states in a random world: Relationship between the nonlinear differential equations of excitability and the stochastic properties of ion channels," *J. Stat. Phys.* **70**, 339–354 (1992).
- <sup>55</sup>A. Pais, *Subtle is the Lord...: The Science and Life of Albert Einstein* (Oxford University Press, Oxford, 1982), pp. 443.
- <sup>56</sup>R. Feldberg, M. Szymkat, C. Knudsen, and E. Mosekilde, "Iterated-map approach to die tossing," *Phys. Rev. A* **42**, 4493–4502 (1990).
- <sup>57</sup>D. Jensen, *Intrinsic Cardiac Rate Regulation* (Appleton-Century-Crofts, New York, 1971).
- <sup>58</sup>A. C. Guyton, *Textbook of Medical Physiology*, 8th ed. (Saunders, Philadelphia, 1991), pp. 218–219.
- <sup>59</sup>G. Parati, M. di Rienzo, S. Omboni, P. Castiglioni, A. Frattola, and G. Mancia, "Spectral analysis of 24 h blood pressure recordings," *Am. J. Hypertens.* **6**, 188S–193S (1993).
- <sup>60</sup>A. Livnat, J. E. Zehr, and T. P. Broten, "Ultradian oscillations in blood pressure and heart rate in free-running dogs," *Am. J. Physiol.* **246**, R817–R824 (1984).
- <sup>61</sup>B. Hoop, H. Kazemi, and L. Liebovitch, "Rescaled range analysis of resting respiration," *Chaos* **3**, 27–29 (1993).
- <sup>62</sup>L. Goodman, "Oscillatory behavior of ventilation in resting man," *IEEE Trans. Biomed. Eng.* **BE-11**, 82–93 (1964).
- <sup>63</sup>T. Wheeler and P. J. Watkins, "Cardiac denervation in diabetes," *Br. Med. J.* **4**, 584–586 (1973).
- <sup>64</sup>C. Vallbona, D. Cardus, W. A. Spencer, and H. E. Hoff, "Patterns of sinus arrhythmia in patients with lesions of the central nervous system," *Am. J. Cardiol.* **16**, 379–389 (1965).
- <sup>65</sup>A. L. Goldberger, D. R. Rigney, J. Mietus, E. M. Antman, and S. Greenwald, "Nonlinear dynamics in sudden cardiac death syndrome: Heart rate oscillations and bifurcations," *Experientia* **44**, 983–987 (1988).
- <sup>66</sup>R. E. Kleiger, J. P. Miller, J. T. Bigger, Jr., A. J. Moss, and the Multicenter Post-Infarction Research Group, "Decreased heart rate variability and its association with increased mortality after acute myocardial infarction," *Am. J. Cardiol.* **59**, 256–262 (1987).
- <sup>67</sup>E. H. Hon and S. T. Lee, "Electronic evaluation of the fetal heart rate," *Am. J. Obstet. Gynecol.* **87**, 814–828 (1963).
- <sup>68</sup>M. Pagani, F. Lombardi, S. Guzzetti, O. Rimoldi, R. Furlan, P. Pizzinelli, G. Sandrone, G. Malfatto, S. Dell'Orto, E. Piccaluga, M. Turiel, G. Baselli, S. Cerutti, and A. Malliani, "Power spectral analysis of heart rate and arterial pressure variabilities as a marker of sympatho-vagal interaction in man and conscious dog," *Circ. Res.* **59**, 178–193 (1986).
- <sup>69</sup>D. T. Kaplan, M. I. Furman, S. M. Pincus, S. M. Ryan, L. A. Lipsitz, and A. L. Goldberger, "Aging and the complexity of cardiovascular dynamics," *Biophys. J.* **59**, 945–949 (1991).
- <sup>70</sup>A. J. S. Coates, J. Conway, P. Sleight, T. E. Meyer, V. K. Somers, J. S. Floras, and J. V. Jones, "Interdependence of blood pressure and heart period regulation in mild hypertension," *Am. J. Hypertens.* **4**, 234–238 (1991).
- <sup>71</sup>G. Mancia, A. Ferrari, L. Gregorini, G. Parati, G. Pomidossi, G. Bertinieri, G. Grassi, M. di Rienzo, A. Perdotti, and A. Zanchetti, "Blood pressure and heart rate variabilities in normotensive and hypertensive human beings," *Circ. Res.* **53**, 96–104 (1983).
- <sup>72</sup>R. Pool, "Is it healthy to be chaotic?," *Science* **243**, 604–607 (1989).
- <sup>73</sup>C. S. Ito and A. M. Scher, "Hypertension following arterial baroreceptor denervation in the unanesthetized dog," *Circ. Res.* **48**, 576–586 (1981).
- <sup>74</sup>G. Mancia, G. Parati, G. Pomidossi, R. Casadei, M. di Rienzo, and A. Zanchetti, "Arterial baroreflexes and blood pressure and heart rate variabilities in humans," *Hypertension* **8**, 147–153 (1986).
- <sup>75</sup>J. P. Zbilut, G. Mayer-Kress, P. A. Sobotka, M. O'Toole, and J. X. Thomas, Jr., "Bifurcations and intrinsic chaotic and  $1/f$  dynamics in an isolated perfused rat heart," *Biol. Cybern.* **61**, 371–378 (1989).
- <sup>76</sup>M. R. Guevara, L. Glass, and A. Shrier, "Phase locking, period-doubling bifurcations, and irregular dynamics in periodically stimulated cardiac cells," *Science* **214**, 1350–1353 (1981).
- <sup>77</sup>J. Hescheler and R. Speicher, "Regular and chaotic behavior of cardiac cells stimulated at frequencies between 2 and 20 Hz," *Eur. Biophys. J.* **17**, 273–280 (1989).
- <sup>78</sup>R. Kapral, "Stochastic dynamics of limit-cycle oscillators with vulnerable phases," *J. Chim. Phys.* **84**, 1295–1303 (1987).
- <sup>79</sup>T. R. Chay and H. S. Kang, "Role of single-channel stochastic noise on bursting clusters of pancreatic  $\beta$ -cells," *Biophys. J.* **54**, 427–435 (1988).
- <sup>80</sup>A. Sherman, J. Rinzel, and J. Keizer, "Emergence of organized bursting in clusters of pancreatic  $\beta$ -cells by channel sharing," *Biophys. J.* **54**, 411–425 (1988).